

Received April 2, 2020, accepted April 17, 2020, date of publication April 21, 2020, date of current version May 5, 2020.

Digital Object Identifier 10.1109/ACCESS.2020.2989167

# Research on the GIC Governance Scheme of the Xinjiang 750-kV Power Grid Based on an Equal Allocation Method

SHU-MING ZHANG<sup>1</sup> AND LIAN-GUANG LIU, (Member, IEEE)

State Key Laboratory of Alternate Electrical Power System with Renewable Energy Sources, North China Electric Power University, Beijing 102206, China

Corresponding author: Shu-Ming Zhang (interzsm@ncepu.edu.cn)

This work was supported in part by the National Natural Science Foundation of China under Grant 51577060, in part by the National High Technology Research and Development of China through the 863 Program under Grant 2012AA121005, and in part by the International Science and Technology Cooperation Program under Grant 2010DFA64680.

**ABSTRACT** The damage caused to power grid by geomagnetic storm increases with an increase in the grid voltage level and an increase in the grid coverage area. Xinjiang is a vast, high-latitude area in China, where geomagnetically induced currents (GIC) have an enormous effect on geomagnetic storm. The voltage level of the Xinjiang power grid (750 kV) and the DC resistance of the grid are small, which aggravates the impact of GICs on the power grid. During geomagnetic storm, the safety and stability of the Xinjiang power grid is crucial. But Xinjiang power grid supplies power for a large range of area, and the grid structure is mostly connected by single transmission line. Therefore, the power grid is relatively weak in resisting accidents and has high operational risk. In this paper, Xinjiang's 750-kV power grid was chosen as a research object, and a GIC governance method (a shared governance method) is proposed. The Xinjiang power grid's control over GIC effects was analyzed, and the effectiveness of the method was verified using simulations.

**INDEX TERMS** Xinjiang power grid, 750-kV, GIC governance, sharing method.

## I. INTRODUCTION

Geomagnetic storms can negatively influence grounded systems across the globe. The harm caused by geomagnetic storms to power grids is a widespread concern. The effects of geomagnetic storms on power grids are mainly reflected in the phenomenon of DC bias caused by geomagnetically induced currents (GICs) [1], [2]. The magnitude of GICs in a particular network is affected by the intensity of the geomagnetic storm, the Earth's conductivity, and the orientation and makeup of the power grid. Generally, areas of higher latitude will see larger variations in the Earth's geomagnetic field, leading to larger GICs. In addition, the smaller the Earth's conductivity, the larger the induced geoelectric fields will be. These drive GICs in grounded networks. Depending on the area, the size and voltage level of the grid will have a significant effect on the magnitude of GICs. As the scale of a network is increased, power grids will tend to be greater affected by GICs [3], [4]. Many geomagnetic storms have encroached on power grids in many parts of northern Europe

The associate editor coordinating the review of this manuscript and approving it for publication was Lin Zhang<sup>2</sup>.

and North America at high latitudes. The most serious ones have caused blackouts in Quebec, Canada, and in Malmo, Sweden [5]–[7]. With the development of China's economy, the scale of China's power grid is also expanding. In recent years, the speed of China's power grid construction has been very impressive, and the scale of power grid development is rapid. With the expansion of China's power grid, there have been several incidents involving magnetic storm. For example, during a magnetic storm in November 2004, a maximum GIC value of 75.5 A was measured in a 500-kV transformer's neutral point at Guangdong Lingao nuclear power station [8]. The Jiangsu power grid and the Heilongjiang power grid have also suffered different degrees of geomagnetic storm. China's northwest region is more influenced by such storms due to its high latitude, relative to the rest of China [9], [10]. China's northwest region is more influenced by such storms due to its high latitude [10]. A 750-kV power grid voltage level is widely used across Northwest China: 750-kV transmission lines use 400-mm<sup>2</sup> six-split conductors, a DC resistance of 2/3, and 400-mm<sup>2</sup> transmission lines with four 400-mm<sup>2</sup> wires. Due to these factors, the 750-kV Xinjiang power grid has one of the largest GIC values in China. Studying the

prevention and control of geomagnetic storm in the Xinjiang power grid is of great significance not only to ensure the structural integrity of the Xinjiang power grid, but also to provide theoretical support for large-scale power grid accident prevention.

The traditional DC bias control method is based on the calculated results of simulated GICs. Capacitance is added in the transformer’s neutral point of the substation with large GICs. By blocking the DC characteristics of the capacitor-governing device, the GIC flow path is blocked, thus limiting the GIC value of the substation [11]. However, this may drive the GIC of the substation with the control device into nearby substations, thus increasing the GIC level of the surrounding substations [12]–[14]. This problem will not arise if a resistance control device is installed. After adding resistance, the DC resistance of the power system will increase, and the GIC value of the whole power grid will be reduced. This type of governance is more secure and reliable. However, with some nodes, it is not effective to install resistance control devices. Therefore, considering the overall power grid, this paper puts forward a theoretical resistance-type device which is installed at the neutral point of the transformer in several substations, and reduces the GICs in the whole power grid by means of sharing the GICs in several substations, thus limiting the GICs level of the entire power grid. This paper takes Xinjiang’s 750-kV power grid as a research object and analyzes the GIC level of the Xinjiang power grid using idealized geoelectric fields and GIC calculations. This paper puts forward a method to mitigate geomagnetic effects in Xinjiang’s 750-kV power grid: the method uses all of the grid’s transformer nodes to share the GICs across the power grid and thus limit the GIC level of each station in the network. For this proposed governance plan, Matlab software was used to carry out the simulations. The GIC-Q reactive power loss method using a K-value was used to calculate the size of the GIC-Q before and after treatment. By comparing and analyzing the GIC level and GIC-Q size before and after treatment, the feasibility of the control scheme was verified, and new ideas for accident prevention in other large-scale power grids are provided.

**II. EQUIVALENT GRID MODEL AND CALCULATION METHOD FOR GIC CALCULATION**

**A. EQUIVALENT MODEL AND PARAMETERS OF THE POWER GRID**

In this paper, Xinjiang’s 750-kV power grid was selected as a research object. The structure of the Xinjiang 750-kV power grid is shown in Figure 1. Up to now, the Xinjiang power grid has a power supply range of more than 1.3 million square kilometers, including 19 750-kV substations, 28 transformers, and a total substation capacity of 41000MVA. There are 35 750-kV lines, and the length of Xinjiang is 6133.28km. We selected 19 750-kV substations on which to conduct the research. It can be seen from the structure of the Xinjiang power grid that it is large in scale, long in terms of

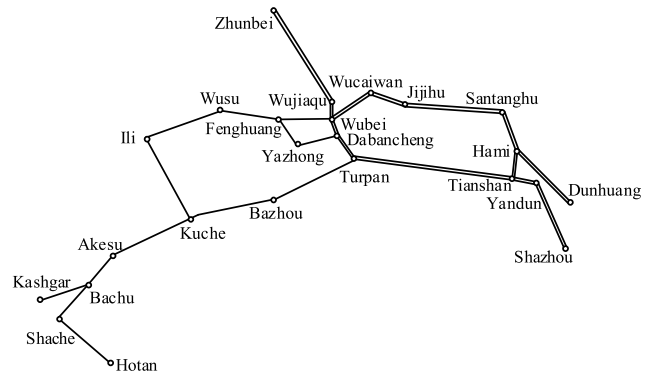


**FIGURE 1. Xinjiang’s 750-kV power network structure diagram.**

**TABLE 1. Parameters of substation, transformer and transmission circuit.**

Transformer series winding (Ω)	Transformer common winding (Ω)	Grounding resistance of Substation (Ω)	Resistance of transmission lines (Ω/km)
0.158465	0.007935	0.3	0.01205

transmission lines, and complex in terms of its power network structure. It contains two East and West ring networks around the Tianshan Mountains. The east ring network covers the main energy base of Xinjiang. In order to ensure the outward transmission of power, the power grid mainly adopts a double-loop network connection mode. The Western ring network mainly covers big cities such as Urumqi and Changji (generally residential electricity). Since the reliability of the power supply in the past was not high, a single-loop network was also adopted. At present, the main grid structure of the Xinjiang power grid is concentrated in the northern part of Xinjiang, and the grid structure is mostly connected by single transmission line. Therefore, the power grid is relatively weak in resisting accidents and has high operational risk. When a geomagnetic storm occurs, the risk to the weak grid structure is lower, which is the reason why we chose the Xinjiang power grid for this research.

For this study, we used unified parameters of transformer parameters and the transmission line parameters of different 750-kV substations in Xinjiang’s power grid. The parameters are shown in Table 1. The numbers of transformers in 750kV substation are shown in Table 2.

Although the lower voltage level power grid has a great impact on the GICs value of the higher voltage level power grid [20], for the special voltage sequence of 750-kV in Xinjiang, the voltage difference between the main grid structure and the lower level power grid is large, and the impact of the lower level power grid can be ignored. In order to illustrate the problem, we only discuss 750-kV voltage level substations and their transmission lines as research objects, ignoring the GIC flowing into the 750-kV power grid through the 220-kV voltage level grid and assuming a uniform approximate equivalence for 750-kV transformers from different manufacturers. The model used in this paper regards transformer winding

TABLE 2. The number of 750kV transformers.

Substation	Number	Substation	Number
Hotan	2	Yazhong	1
Shache	2	Dabancheng	1
Kashgar	2	Wubei	2
Bachu	1	Turpan	1
Akesu	1	Wujiaqu	1
Kuqa	2	Zhunbei	1
Ili	1	Wucaiwán	2
Bazhou	1	Jijihu	2
Wusu	1	Tianshan	1
Fenghuang	1		

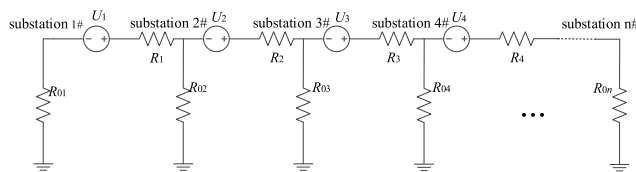


FIGURE 2. Equivalency model of the geomagnetically induced current (GIC) power grid.

and transformer grounding resistance as a series of resistances. An equivalency model of the power grid is shown in Figure 2.

When establishing an equivalency model of transmission lines, a three-phase balance is generally assumed, that is, resistance can be equivalent to the parallel connection of three phase lines. For double-circuit transmission lines, the resistance can be equivalent to the parallel connection of double-circuit transmission lines. Because the grounding resistance of a grounding wire through a tower is far greater than the earth resistance of a transmission line, this remains approximately uniform in the calculation of GICs, so the calculation of the grounding of a lightning conductor was not done for this paper.

### B. GIC AND GIC-Q COMPUTING METHODS

In order to simplify the calculation process, the induction voltage source of the line was calculated as follows. The eastern induced electric field and the northern induced electric field were both set as 1-V/km homogeneous geoelectric fields [15], which is a typical value used for calculating GICs:

$$U_{ij} = E_N L_{ijN} + E_E L_{ijE} \quad (1)$$

The equations for  $E_N$  and  $E_E$  are for the northern and eastern electric fields, respectively, and the units are in V/km.  $L_{ijN}$  and  $L_{ijE}$  are the Northern equivalent length and Eastern equivalent length, respectively, of the transmission lines. According to Thevenin's equivalent theorem, the line-induced voltage source is converted into an equivalent current source in the following form:

$$I_i = \sum g_{ij} U_{ij} = \left( \sum g_{ij} L_{ijN} \right) E_N + \left( \sum g_{ij} L_{ijE} \right) E_E \quad (2)$$

$$\mathbf{I} = [I_1, I_2 \dots I_n] = \mathbf{H}\mathbf{E} \quad (3)$$

Here,  $g_{ij}$  is the three-phase conductance value of the transmission line:

$$g_{ij} = 1/R_{ij}$$

$$\mathbf{H} = \begin{bmatrix} \sum_{j=1}^n g_{1j} L_{1j}^N & \sum_{j=1}^n g_{1j} L_{1j}^E \\ \sum_{j=1}^n g_{2j} L_{2j}^N & \sum_{j=1}^n g_{2j} L_{2j}^E \\ \dots & \dots \\ \sum_{j=1}^n g_{nj} L_{nj}^N & \sum_{j=1}^n g_{nj} L_{nj}^E \end{bmatrix}_{n \times 2}$$

$$\mathbf{E} = \begin{bmatrix} E^N \\ E^E \end{bmatrix}_{2 \times 1}$$

According to the circuit solution method, the node voltage is obtained:

$$\mathbf{V} = [V_1, \dots, V_n]^T = \mathbf{G}^{-1}\mathbf{I} = \mathbf{G}^{-1}\mathbf{H}\mathbf{E}$$

$$\mathbf{G} = \begin{bmatrix} \sum_{j=1}^n g_{ij} + g_1 & -g_{12} & \dots & -g_{n1} \\ -g_{21} & \sum_{j=1}^n g_{2j} + g_2 & \dots & -g_{n2} \\ \dots & \dots & \dots & \dots \\ -g_{n1} & -g_{n2} & \dots & \sum_{j=1}^n g_{nj} + g_n \end{bmatrix}_{n \times n} \quad (4)$$

Finally, the geomagnetically induced current ( $I_{GIC}$ ) of each branch is calculated in a matrix form, as follows:

$$\mathbf{I}_{GIC} = \mathbf{C}_r \mathbf{G}^{-1} \mathbf{H} \mathbf{E} \quad (5)$$

The matrix  $\mathbf{C}_r$  is an  $n \times n$  order matrix. If there is resistance between the corresponding  $i$  and  $j$  nodes, there are only two nonzero elements in the  $\mathbf{C}_r$  matrix. The positions include  $i$  columns and  $j$  columns, and the value is the conductance between nodes  $i$  and  $j$ . The corresponding node is positive, and the outflow node is negative. For the substation's neutral point, there is only one nonzero element in the  $\mathbf{C}_r$  matrix, the location is in the  $i$  column, and the value is the neutral point grounding conductance value.

### C. CALCULATION METHOD FOR GIC-Q

To study the impact of GIC on the power grid, we introduced a  $K$ -value algorithm to calculate the reactive power loss of transformers during geomagnetic storms. In 2001, Dong and others first proposed the  $K$ -value algorithm to calculate the transformer GIC-Q loss [15]: they verified that the GIC-Q loss was directly proportional to the DC current of the transformer neutral point. The GIC-Q loss model for each transformer is as follows:

$$Q_{Loss} = V_{pu} K I_{GIC} \quad (6)$$

TABLE 3. GIC and GIC-Q of substations before treatment.

Number	Substation	GIC (A)	GIC-Q (Mvar)
1	Hotan	85.13	72.36
2	Shache	-146.70	124.7
3	Kashgar	-153.48	130.46
4	Bachu	6.70	5.7
5	Akesu	-9.15	7.78
6	Kuqa	-81.70	69.44
7	Ili	-118.11	100.39
8	Bazhou	90.89	77.25
9	Wusu	-90.22	76.69
10	Fenghuang	-75.66	64.31
11	Yazhong	-43.60	37.06
12	Dabancheng	-13.61	11.57
13	Wubei	-35.08	29.82
14	Turpan	65.41	55.6
15	Wujiaqu	43.16	36.69
16	Zhunbei	-98.91	84.07
17	Wucaiwan	15.60	13.26
18	Jijihu	76.96	65.42
19	Tianshan	109.03	92.67

$Q_{Loss}$  is the GIC-Q loss of the transformer, in Mvar;  $V_{pu}$  is the standard value of the terminal voltage of the transformer while actually being operated;  $K$  is the reactive power loss coefficient of the transformer, in Mvar/A; and  $I_{GIC}$  is the single-phase GIC passing through the transformer winding, in A. The  $K$ -value in the formula usually takes an empirical value, and the  $K$ -value of each type of transformer is known by default. By using the transformer's rated voltage, Equation (6) can be rewritten as follows:

$$Q_{Loss} = V_{pu}K \left( \frac{V_{NomkV}}{V_{NomkV \cdot Assumed}} \right) I_{GIC} \quad (7)$$

Here,  $V_{NomkV}$  is the rated voltage of the high-voltage winding side of the transformer, and  $V_{NomkV \cdot Assumed}$  is 750 kV.

### III. GIC AND GIC-Q ANALYSIS BEFORE GOVERNANCE

The substation and line GIC of the Xinjiang 750-kV power grid are shown in Tables 3, Tables 4 and Figure 3. The calculated GICs are the sum of contributions from the Northward and Eastward components of the electric field. Here,  $E_E$  and  $E_N$  respectively represent the electric field in an eastward and northward direction. The positive and negative GIC in the substation indicate that the GIC flow into and out of the neutral point of the transformer. The line GIC is positive, which means that the direction of GIC flow is consistent with the reference lines in the third column of Table 3; otherwise, it would be inconsistent.

Through the calculations, we can see that in the Shache substation, in the Kashgar substation, in the Ili substation, and in the other substations in the corners of the power grid, GICs flowed into a substation from the surrounding substations. Due to the accumulation of GICs, the GIC values were larger here. The Zhunbei substation and the Hotan substation are at the end of the grid, so the GIC level was relatively large. The results are in line with the basic principles of GIC distribution,

TABLE 4. GIC of transmission lines before treatment.

Electric field	750kV transmission line	Line GIC before treatment /A
Eastward electric field	TS—YD	332.1
	JJH—STH	382.4
	TLF—TS	438.3
	WCW—JJH	352.4
Northward electric field	DBC—TLF	307.3
	TS—YD	-238.7
	JJH—STH	-110.2
	TLF—TS	-159.2
	WCW—JJH	-79.2
	DBC—TLF	-342.6

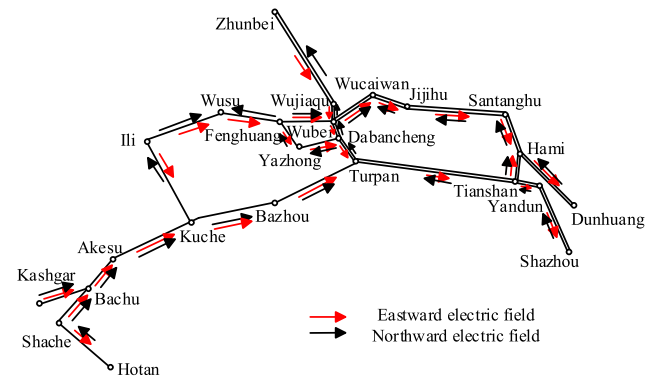


FIGURE 3. GIC flow direction of a 750-kV line in the eastern electric field and northern electric field.

and they also confirmed the inflection effect of GIC distribution. Among the 750-kV transmission lines, we selected five lines with large GIC values for a demonstration. The GIC of the transmission lines in the Eastern electric field and northern electric field are shown in Table 4.

### IV. A METHOD FOR CONTROLLING THE GICS OF POWER GRIDS WITH LOW RESISTANCE

#### A. PHYSICAL MODEL

This paper proposes that the entire network be installed with small resistors to share the GICs across the power grid, thus limiting the GIC level of the entire power grid. A four-node model of a low-resistance grid sharing GIC is shown in Figure 4 [16].

A four-node model is illustrated in Figure 4, where 1, 2, 3, and 4 represent nodes;  $U_{ij}$  ( $i, j = 1, 2, 3, 4$ ) represents line equivalent voltage sources; and  $R_{ij}$  ( $i, j = 1, 2, 3, 4$ ) represents transmission line resistance.  $R_{gi}$  ( $i = 1, 2, 3, 4$ ) represents the equivalent resistance of the transformer winding and the neutral point grounding resistance in a series, and  $R_{ssi}$  ( $i = 1, 2, 3, 4$ ) represents the low resistance of the neutral point connected to the device, which governs the equivalent resistance of the device. Its value can be zero or nonzero. When the value is 0, this indicates that the site is not equipped with a low-resistance control device. When the value is not 0, a low-resistance control device with an equivalent resistance value of  $R_{ssi}$  is added to the site.

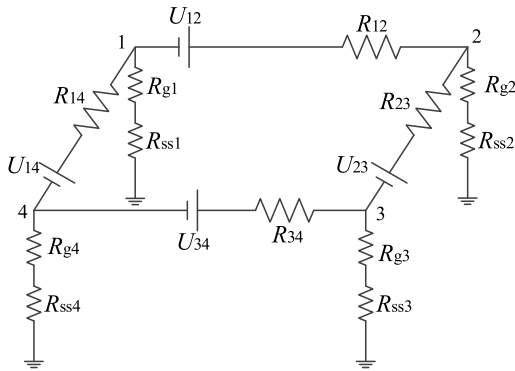


FIGURE 4. A four-node model of GICs sharing low resistance.

## B. MATHEMATICAL MODEL AND ALGORITHM FLOW

The DC bias control scheme should take into account both functional and economic requirements and meet the requirements of relevant technical specifications, so this is a multi-objective optimization problem. In this paper, the elitist nondominated sorting genetic algorithm (NSGA- II) with elitist strategy is used to solve the multi-objective optimization model [17]. The basic idea of NSGA- II algorithm is: first, build the objective function, and then randomly generate the initial population of  $N$ . After the nondominated sorting, the first generation of the subpopulation was obtained through three basic operations of genetic algorithm selection, crossover and mutation. After second generations, the parent and offspring population were merged to make quick non dominated sorting, and the crowding degree of each non dominated layer was calculated. According to the relationship between nondominance and individual crowding, we select excellent individuals to form a new parent population, which preserves the diversity of the population, and also enables the outstanding individuals of the father to enter the next generation. Finally, a new offspring population is generated by genetic algorithm. And so on, until the iterated algebra reaches the maximum iterated algebra, it will exit the cycle and get the final Pareto optimal solution set.

### 1) OBJECTIVE FUNCTION

#### a: OBJECTIVE FUNCTION 1

The small resistance connected by neutral point should ensure the effectiveness and reliability of the transformer grounding, as far as possible meet the requirements of the [18] standard for the grounding of the AC electrical installations, and the resistance of the series connection is as small as possible.

Set the direction of east electric field  $0^\circ$ . And rotate counterclockwise the direction of electric field 180 degrees in 1 degree increments. Set a transmission line with the direction of  $\theta$ . The value of uniform geoelectric field is set 1 V/km. Then GIC in the line can be obtained,

$$I_{GIC} = a \cos \theta + b \sin \theta = A \cos (\theta - \alpha) \quad (8)$$

where

$$\alpha = \arctan (b/a)$$

$$A = (a^2 + b^2)^{1/2}$$

$$a = \frac{E_\theta L_E}{R}$$

$$b = \frac{E_\theta L_N}{R}$$

where  $E_\theta$  represents the geoelectric field along the transmission line.  $\theta$  is the angle between the given electric field direction and the eastward electric field.  $R$  is the total resistance in the circuit. When the known electric field is 1V/km uniform and constant, the maximum value of the geomagnetic induced current of transformer substations in any direction is the following form.

$$I_{\max, \max} = \max (|I_j| = |A_j| ; j = 1, 2, \dots, M) \quad (9)$$

For each transformer node, find the East and north direction of the  $I_{GIC}$ , and then find the minimum value of  $I_{\max, \max}$  as the first optimization objective function, that is

$$\min (I_{\max, \max}) = \min (|A_j|, j = 1, 2, \dots, M) \quad (10)$$

#### b: OBJECTIVE FUNCTION 2

Taking into account the economic principle of equipment installation, it is also necessary to minimize the cost of the control device in order to achieve the goal of governance with fewer pieces of equipment. It is assumed that the same resistance level is adopted in the same voltage class, and the different resistances are regulated by different gears of the device, so the cost is reflected in the quantity of equipment. Then the objective function is

$$\min R_{sum} = \sum_{i=1}^q R_{ssi} \quad (11)$$

In the formula,  $R_{sum}$  represents the resistance value of all small resistance control devices,  $R_{ssi}$  indicates the  $i$  small resistance control device, and the  $q$  indicates the number of governing devices.

Formula 13 and formula 14 constitute the multi-objective optimization function of GIC governance in power grid. However, the above two objectives are contradictory and mutually restrictive, and the better the governance effect is, the smaller the maximum geomagnetic induced current of the neutral point, the more necessary the harnessing device is, and the worse the economy is. The significance of multi-objective optimization is to balance multiple objective functions as far as possible to achieve the global optimal solution when the constraints are satisfied.

### 2) CONSTRAINT CONDITION

#### a: CONSTRAINT 1

Referring to the technical guidelines of HVDC grounding electrode, the research results of document [19] single-phase transformer GIC should not exceed 30A. In references [19], the upper limit of the neutral point current constraint is set to 30A, so the constraint condition of setting neutral current is

$$I_{\max, \max} < 30$$

*b: CONSTRAINT 2*

According to the “grounding design code for AC electrical installations”, and to ensure the validity and reliability of the grounding of transformers, the resistance should be as small as possible in the neutral point of the transformer, and the constraint conditions should be set as

$$0 < R_{ssi} \leq 2.2$$

*c: CONSTRAINT 3*

In order to embody the idea of sharing, the maximum value of the neutral point GIC of the geoelectric field in the range of  $1^\circ \sim 180^\circ$  is  $I_{\max,avg}$  is used as another constraint condition, and the value given by reference [19] determines that the constraint conditions are as follows.

$$I_{\max,avg} = \max \left( \frac{1}{M} \sum_{j=1}^M (|I_{GICnj}|; n = 1, 2, \dots, K) \right) < 20$$

This method can get the Pareto optimal solution by solving the optimization model of power grid GIC, that is, balancing the objective functions to determine the optimal solution. The flow chart of NSGA- II algorithm for small power grid to deal with power grid GIC is shown in Figure 5.

The NSGA- II algorithm is used to solve the problem, and a small resistance configuration scheme in the Pareto optimal solution set is obtained, as shown in table 5. Due to the large number of Pareto optimal solutions, only a few partial options are listed here.

According to the small resistance configuration scheme of Pareto optimal solution set in table 6 and the Pareto optimal solution set of figure 6, we can see that the two objective functions restrict each other, increasing the total resistance value of configuring small resistance can reduce the maximum value of single phase GIC, and the optimal solution set reflects the mutual balance between economy and effectiveness. According to the optimization results of NSGA-II algorithm in Figure 6, when the number of iterations reaches 70, the maximum value of GIC at the neutral point is close to 30A. The maximum value decreased slowly, and finally stabilized at 25.19A. The calculated optimal scheme is shown in Table 4-2. The small resistance is used to optimize the GIC scheme of Xinjiang 750kV power grid. The total resistance of the optimized configuration is 19, the maximum current  $I_{\max,max}$  and the maximum value  $I_{\max,avg}$  of the average GIC of the neutral point are 29.83A and 12.83a respectively and the total resistance of the small resistance is 25.50Ω.

By increasing the DC impedance of the DC impedance network of the power system, the GIC level could be reduced, and the GIC level of each node within the system could effectively be limited through the sharing of GICs throughout the entire network.

**C. OPTIMIZATION RESULTS AND ANALYSIS**

In accordance with the low resistance given in Table 6, the GIC in Xinjiang’s 750-kV power grid were optimized,

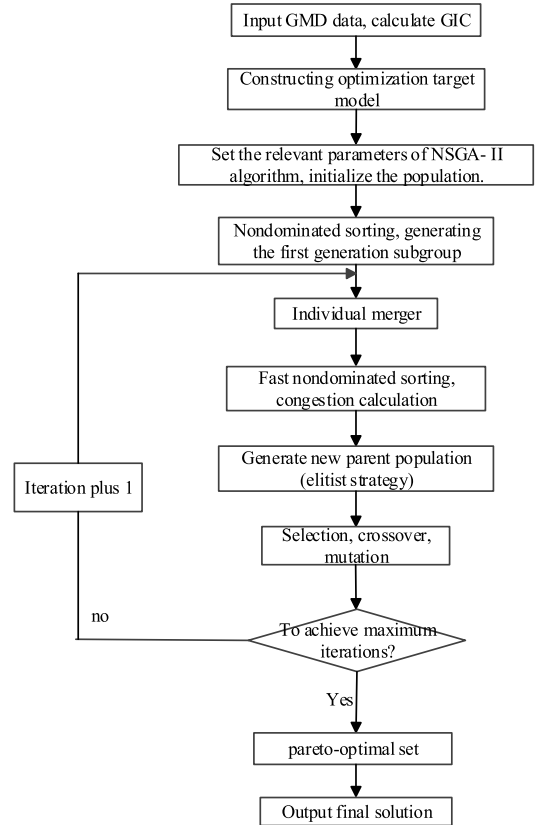


**FIGURE 5. NSGA-II algorithm flowchart.**

**TABLE 5. Pareto optimal solution centralized small resistance configuration scheme.**

pareto-optimal set	Total number of small resistors	min $R_{sum}$ (Ω)	min $I_{\max,max}$ (A)	$I_{\max,avg}$ (A)
1	19	25.87	29.95	13.11
2	19	25.81	29.93	12.95
3	19	25.66	29.23	13.31
4	19	25.55	29.07	13.24
5	19	25.50	29.83	12.83
6	19	25.42	29.35	13.35
7	19	25.41	29.51	13.51
8	19	25.24	29.47	13.47
9	19	25.24	29.61	13.61
10	19	25.19	29.78	13.78

and the GIC of the grid before and after optimal resistance management were calculated, as shown in Table 6. Further, the GIC values before and after the comparison were calculated as well. The GIC in the table are positive. The direction of the GIC indicates how the currents flowed from the neutral point of the transformer into the grid. If the GICs are negative, this indicates that the GIC flowed into the earth from the neutral point of the transformer. In Table 7, we can see that after adopting the sharing method to control the GICs of the 750-kV Xinjiang power grid, the GIC in the entire network decreased significantly. The maximum reduction of geomagnetic induction current on the transmission line is 65A. As is shown in Figure 6, by using a low-resistance

**TABLE 6.** GIC scheme for Xinjiang 750kV power grid based on resistance method.

Serial number	Substation	Resistance value of resistors
1	Hotan	1.94
2	Shache	2.31
3	Kashgar	2
4	Bachu	0.76
5	Akesu	0.34
6	Kuqa	1.57
7	Ili	1.61
8	Bazhou	0.83
9	Wusu	1.71
10	Fenghuang	1.2
11	Yazhong	2.24
12	Dabancheng	0.42
13	Wubei	0.23
14	Turpan	1.53
15	Wujiaqu	1.53
16	Zhunbei	1.55
17	Wucaiwán	0.54
18	Jijihu	1.81
19	Tianshan	1.38

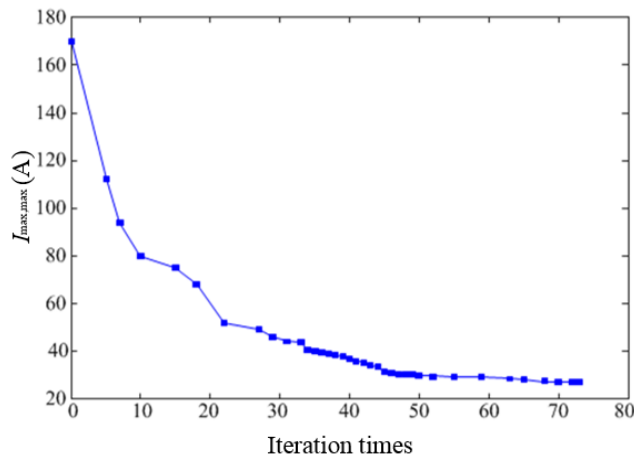


**FIGURE 6.** Pareto-optimal set.

device to control the DC network topology and effectively redistribute the GIC of the entire network, the GIC could be shared. This means that, especially in sites at high risk for power grid geomagnetic storm, optimization treatment could significantly reduce the site’s GIC, such as in the Shache substation or Kashgar substation.

Taking Xinjiang’s 750-kV power grid as the research object, we established a GIC-Q loss model for transformers in Xinjiang’s 750-kV substations both before and after optimization with low resistance. Further, the GIC-Q of Xinjiang’s 750-kV power grid was calculated before and after optimal resistance management. The GIC-Q was calculated only for effect verification, so the  $V_{pu}$  approximate value was 1 and the K-value was 1.7. A comparison diagram of the transformers in Xinjiang’s 750-kV substations is shown in Table 7 and Figure 7 before and after optimization treatment, respectively. The calculated GICs are the sum of contributions from the Northward and Eastward components of the electric field.

**TABLE 7.** Xinjiang 750 kV transmission line GIC before and after treatment.

Electric field	750kV transmission line	Line GIC before treatment	Line GIC after treatment	Difference of GIC/A
		/A	/A	
Eastward electric field	TS—YD	332.1	246.7	-85.4
	JJH—STH	382.4	348.4	-34.0
	TLF—TS	438.3	411.1	-27.2
	WCW—JJH	352.4	336.5	-15.9
	DBC—TLF	307.3	296.0	-11.3
Northward electric field	TS—YD	-238.7	-221.6	-17.1
	JJH—STH	-110.2	-133.8	23.7
	TLF—TS	-159.2	-118.9	-40.3
	WCW—JJH	-79.2	-90.4	11.2
	DBC—TLF	-342.6	-328.0	-14.6

**TABLE 8.** GIC and GIC-Q OF substations after treatment.

Serial number	Substation	GIC (A)	GIC-Q (Mvar)
1	Hotan	42.74	36.33
2	Shache	-42.82	36.4
3	Kashgar	-37.79	32.12
4	Bachu	34.59	29.41
5	Akesu	-16.18	13.75
6	Kuqa	-34.06	28.95
7	Ili	-3.40	2.89
8	Bazhou	2.70	2.29
9	Wusu	-12.13	10.31
10	Fenghuang	-15.25	12.97
11	Yazhong	-2.00	1.7
12	Dabancheng	-5.06	4.3
13	Wubei	-33.75	28.69
14	Turpan	6.15	5.23
15	Wujiaqu	25.99	22.09
16	Zhunbei	-29.39	24.99
17	Wucaiwán	42.53	36.15
18	Jijihu	40.17	34.15
19	Tianshan	10.51	8.93

According to the treatment effects comparison shown in Tables 3 and 8, it can be seen that the substation with the largest GIC value in the former Xinjiang power grid was the Kashgar substation, with 153.48 A, and the substation with the largest GIC value after treatment was the Shache substation, with 42.82 A. The GICs of the entire grid fell below the target value, so the goal of optimizing governance was achieved. According to Table 6, the GIC-Q loss in Xinjiang’s 750-kV power grid after optimization with low resistance was much lower than before optimization. After treatment, the maximum GIC-Q of the whole grid was reduced from 130.46 Mvar in the Kashgar substation to 36.40 Mvar in the Shache substation. The treatment plan reduced the GIC-Q loss at high-risk sites before treatment, such as in the Shache substation and Kashgar substation. In Figure 6, we can see that the GIC-Q loss increased and decreased before and after treatment; however, the overall GIC-Q loss was reduced, and the GIC-Q loss in all stations across the entire network was smaller. By comparing the derivative effects of GIC-Q loss to those of GIC loss, we could fully demonstrate the control

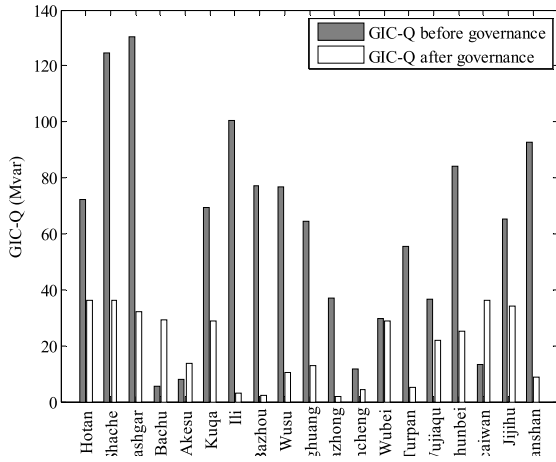


FIGURE 7. Comparison of the GIC-Qs of the transformers in Xinjiang's 750-kV substations before and after treatment.

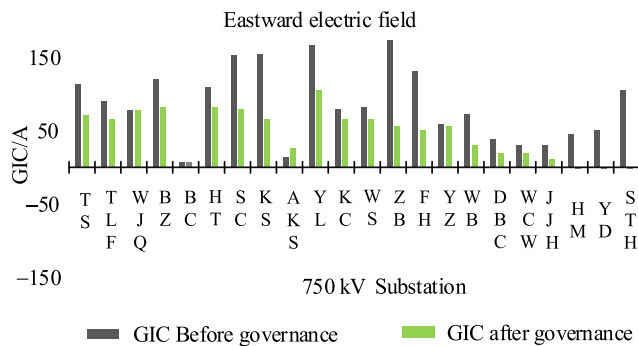


FIGURE 8. GIC comparison of Xinjiang's 750-kV substations before and after EW electric field treatment.

effects of the optimized treatment scheme on damage from geomagnetic storm in Xinjiang's 750-kV power grid.

The secondary reactive power fluctuation of GIC in secondary transformers, which flow through the neutral point into the transformers, threatens the structural integrity of large-scale power grids. Therefore, we paid a lot of attention to the changes in GIC in the neutral points of the transformers. Figures 8 and 9 show a comparison between the neutral point GICs in the transformer stations in the Eastern and northern directions before and after treatment. Transformer GIC only take numerical values and do not consider direction.

As shown in Figures 8 and 9, after treatment, the GIC values at four substations' neutral point have obvious changes under the condition of eastward electric field. Tianshan converter station and in the Turpan substation increased in by 16.4 A and 13.2 A, respectively. There were reduced GIC values in the Jijihu substations and Wucaiwan substations, and the reductions were by 18.1 A and 9.8 A, respectively. In the four substations with large GIC values in the northern electric field, the GIC variation increased in the Jijihu substation, Wucaiwan substation, and Tianshan converter station by 12.4, 6.5, and 4.6 A, respectively. In the Turpan substation, the decrease was 3.6 A.

In Xinjiang 750kV power grid, regardless of the direction of the electric field, the substation with large variation in GICs is located near the one or two level of the substation

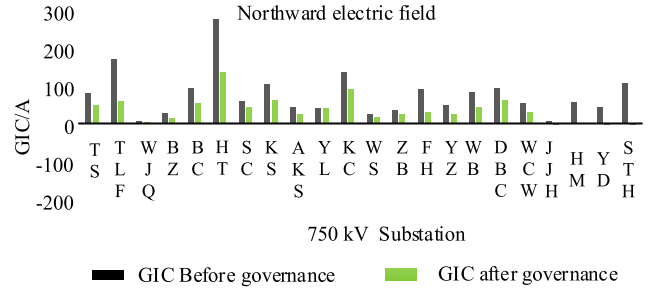


FIGURE 9. GIC comparison of Xinjiang's 750-kV substation before and after Northward electric field treatment.

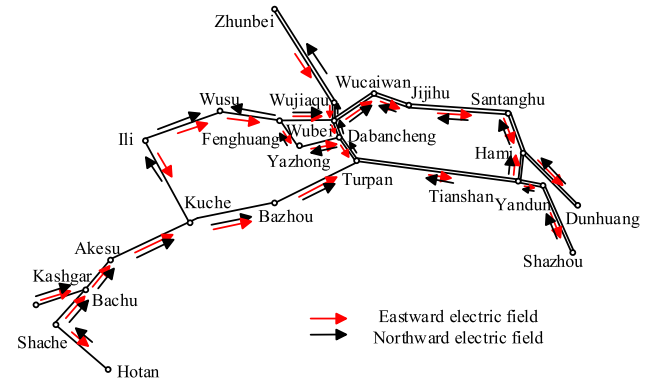


FIGURE 10. GIC flow direction of the 750-kV transmission lines after treatment in the East-to-east electric field and northern electric field.

being controlled. This proved that the influence of DC bias on power grid GICs is regional. In addition, the GIC value of the neutral point in the Tianshan converter station reached 99.3 A in the eastern electric field, far exceeding the allowable DC current limit at the neutral point of a single transformer. This phenomenon is worth paying attention to. The grounding pole bias control may have caused the GIC of the converter station to increase, so that a substation with an original neutral point DC current that met standards became a high-risk substation.

Here, we created an image of the GIC flow direction of the transmission lines in Xinjiang's 750-kV power grid within the eastern electric field and northern electric field. As is shown in Figure 10, the flow direction of the power grid did not change after the sharing of electricity. In Table 6, we list the 750-kV lines with a GIC difference greater than 10 A (before and after treatment), where the GIC line is positive, indicating that the actual direction of the current was consistent with the reference directions in Table 6 (the second column). The differences in the GIC before and after treatment are indicated, where negative values indicate a decrease in the value. According to the calculation results, the reduction in the GIC in the transmission lines running from the Tianshan converter station to the Yandun substation was the most obvious, because the Yandun substation is an important connection node between the Xinjiang power grid and the Gansu power grid. The results due to this treatment were very favorable, which proves the superiority of our control plan.

The variation of GIC in Xinjiang 750-kV substation before and after treatment with the north electric field is larger than that in the east electric field. This is independent of the GIC



itself in the station, and the site is concentrated near the control station. The GICs in the transformers were larger in the Ili substation and Shache substation than in the Wucaiwan substation (all in the northern electric field). The above conclusion is consistent with the idea that GMDs generate a geoelectric field and act on a grid to generate GICs, and it also verifies the inevitability of the inflection effect. As can be seen from Table 6, the 750-kV lines with large GIC variations before and after treatment all had Hami or adjacent lines. This shows that the influence of bias treatment on the GICs of 750-kV transmission lines is regional. Since the direction of the geomagnetic induced current is along the electric field direction, the GIC changes on the transmission lines are more obvious under the east electric field after taking the control measures, while the GICs changes on the transmission lines are not obvious under the action of the north electric field.

## V. CONCLUSION AND DISCUSSION

In this paper, the 750-kV power grid in Xinjiang, China, was chosen as the research object. The influence of geomagnetic storm on Xinjiang's 750-kV power grid was studied through calculation and analysis. In this paper, we suggest the installation of a DC bias control resistance device in the neutral point of transformers at substations in the power grid, and used the method of equal allocation to restrict the GIC level of the power grid. The effectiveness of the method was verified through simulations. The main conclusions are as follows:

- 1) The reasonable installation of resistance management devices in substations of a power grid can effectively limit the GIC level of the power grid. Further, this does not cause the GIC value of some nodes in the power grid to rise due to changes in the DC resistance of the grid, which is safe and efficient;
- 2) This paper proposes an elitist NSGA-II with elitist strategy. Through simulation, the Pareto optimal solution set is obtained and the final optimization scheme is obtained. The method proposed in this paper can effectively reduce the reactive power loss caused by GICs in a power grid and can clearly reduce GIC-Q. In this way, the reactive balance pressure of the power grid during a geomagnetic storm can be effectively reduced, the reactive power balance of the power grid can be guaranteed, and a voltage collapse within the power grid can be effectively prevented;
- 3) Through simulations, the inflexion effect of GIC distribution in the power grid was verified. The GICs in all of the transmission lines flowed along the direction of the electric field. Because the inflexion of the power grid gathered the current in two directions, the GICs of the transformer neutral points in the substations were larger (e.g., in the Shache substation and Ili substation within the eastern electric field, and in the Wucaiwan substation within the northern electric field). The above conclusions are consistent with the idea that GMDs generate geoelectric fields and act on the grid to

generate GICs, which verifies the inevitability of the inflection effect.

## REFERENCES

- [1] J. G. Kappenman and V. D. Albertson, "Bracing for the geomagnetic storms," *IEEE Spectr.*, vol. 27, no. 3, pp. 27–33, Mar. 1990.
- [2] J. G. Kappenman, S. R. Norr, G. A. Sweezy, D. L. Carlson, V. D. Albertson, J. E. Harder, and B. L. Damsky, "GIC mitigation: A neutral blocking/bypass device to prevent the flow of GIC in power systems," *IEEE Trans. Power Del.*, vol. 6, no. 3, pp. 1271–1281, Jul. 1991.
- [3] C. Liu, J. Lin, X. Wang, Z. Wang, and X. Yang, "An optimal layout method of capacitances and resistances for suppressing geomagnetically induced currents in power grid," (in Chinese), *Power Syst. Technol.*, vol. 42, pp. 1681–1686, 2018.
- [4] K. Zheng, L. G. Liu, H. Y. Ge, and W. X. Li, "Comparative study of the GIC amplitudes and characteristics in different power grids in China," in *Proc. 44th CIGRE Session Tech. Exhib.*, Paris, France, 2012, pp. 1–8.
- [5] R. Horton, D. Boteler, T. J. Overbye, R. Pirjola, and R. C. Dugan, "A test case for the calculation of geomagnetically induced currents," *IEEE Trans. Power Del.*, vol. 27, no. 4, pp. 2368–2373, Oct. 2012.
- [6] R. Pirjola and A. Viljanen, "Complex image method for calculating electric and magnetic fields produced by an auroral electrojet of finite length," *Annales Geophysicae*, vol. 16, pp. 1434–1444, Nov. 1998.
- [7] V. Albertson, J. Kappenman, N. Mohan, and G. Skarbakka, "Load-flow studies in the presence of geomagnetically-induced currents," *IEEE Trans. Power App. Syst.*, vol. PAS-100, no. 2, pp. 594–607, Feb. 1981.
- [8] L. Liu, C. Liu, and B. Zhang, "Effects of geomagnetic storm on UHV power grids in China," (in Chinese), *Power Syst. Technol.*, vol. 33, no. 11, pp. 1–5, 2009.
- [9] L. Liu, K. Wang, S. Guo, K. Zheng, K. Wei, C. Liu, Z. Wang, and B. Dong, "Characteristics of GIC interaction in a dual-voltage-level power network," (in Chinese), *Sci. China Technol.*, vol. 45, no. 12, pp. 1311–1320, 2015.
- [10] K. Zheng, L. Liu, D. H. Boteler, and R. J. Pirjola, "Modelling geomagnetically induced currents in multiple voltage levels of a power system illustrated using the GIC-benchmark case," (in Chinese), *Proc. CSEE*, vol. 33, no. 16, pp. 179–186, 2013.
- [11] C. Liu, C. Huang, and M. Pan, "Optimal configuration of capacitor blocking devices for suppressing DC Bias in transformers," (in Chinese), *High Volt. Eng.*, vol. 42, no. 7, pp. 2308–2314, 2016.
- [12] C. Liu, Y. Li, and R. Pirjola, "Observations and modeling of GIC in the Chinese large-scale high-voltage power networks," *J. Space Weather Space Climate*, vol. 4, p. A03, 2014.
- [13] P. Yang, X. Zheng, L. Liu, C. M. Liu, and C. L. Ma, "Effects of transformer neutral grounding via small resistor on mitigating geomagnetically induced currents in power grid," *Power Syst. Technol.*, vol. 41, no. 4, pp. 1324–1331, 2017.
- [14] L. Liu, S. Guo, and K. Wei, "Calculation of geomagnetically induced currents in interconnected north China-central China-east China power grid based on full-node GIC model," (in Chinese), *Power Syst. Technol.*, vol. 38, no. 7, pp. 1946–1952, 2014.
- [15] C. M. Liu, Y. L. Li, and L. Chen, "Modelling geomagnetically induced currents in Xinjiang 750 kV power grid in China," in *Proc. IEEE Power Energy Soc. Gen. Meeting (PES)*, Vancouver, BC, Canada, Jul. 2013, pp. 1–5.
- [16] N. Takasu, T. Oshi, F. Miyawaki, S. Saito, and Y. Fujiwara, "An experimental analysis of DC excitation of transformers by geomagnetically induced currents," *IEEE Trans. Power Del.*, vol. 9, no. 2, pp. 1173–1182, Apr. 1994.
- [17] W. Zezhong, T. Ruijuan, and Z. Ying, "Calculation of no-load DC bias for UHV transformers based on series resistance," (in Chinese), *Acta Electrotech. Sinica*, vol. 32, pp. 129–137, 2017.
- [18] N. Srinivas and K. Deb, "Multiobjective function optimization using non-dominated sorting genetic algorithms," *IEEE Trans. Evol. Comput.*, vol. 2, no. 3, pp. 1301–1308, 1994.
- [19] W. Yuhong, L. Lin, and Z. Chao, "Research on DC bias suppression measures based on several different transformers," *High Voltage Electr. Appliances*, (in Chinese), vol. 53, pp. 159–165, 2017.
- [20] S. P. Blake, P. T. Gallagher, J. Campaña, C. Hogg, C. D. Beggan, A. W. P. Thomson, G. S. Richardson, and D. Bell, "A detailed model of the Irish high voltage power network for simulating GICs," *Space Weather*, vol. 16, no. 11, pp. 1770–1783, Nov. 2018.

•••